

## Effect of fiber and aggregate size on mode-I fracture parameters of high strength concrete

Ch.Naga Satish Kumar\*, P.V.V.S.S.R. Krishna and D.Rohini Kumar

*Department of Civil Engineering, Bapatla Engineering College, Bapatla-522101, India*

*(Received June 27, 2017, Revised September 25, 2017, Accepted September 27, 2017)*

**Abstract.** In this paper, an experimental investigation was carried out to study the effect of volume fraction of fiber and maximum aggregate size on mode-I fracture parameters of high strength concrete. Total of 108 beams were tested on loading frame with three point loading, the variables in the high strength concrete beams are aggregate size (20 mm, 16 mm and 10 mm) and volume fraction of fibers (0%, 0.5%, 1% and 1.5%). The fracture parameters like fracture energy, brittleness number and fracture process zone were analyzed by the size effect method (SEM). It was found that fracture energy ( $G_f$ ) increases with increasing the Maximum aggregate size and also increasing the volume of fibers, brittleness number ( $\beta$ ) decreases and fracture process zone (CF) increases.

**Keywords:** high strength concrete; mode I fracture energy; fracture process zone; brittleness number; steel fiber

### 1. Introduction

The safety and durability of concrete structures is significantly influenced by the cracking behavior of concrete. In order to understand the cracking behavior of concrete, it is necessary to understand the fracture properties of concrete. The study of post peak response of concrete is required to fully understand the failure criterion of concrete, which is based on the fracture parameters i.e., fracture energy of concrete, brittleness number and fracture process zone.

Quasi brittle materials like concrete have low tensile strength and strain capacity. These essential properties of concrete can be enhanced by the inclusion of short discrete steel fibers into the concrete matrix. The augmentation of Steel fibers significantly improves the engineering properties of concrete like the flexural-tensile strength and fracture toughness, thereby retarding or preventing initiation, propagation, and coalescence of cracks (Okan *et al.* 2016, Nardino *et al.* 2010, Holschemacher *et al.* 2010). Upon hardening, the randomly distributed Steel fibers which are bonded in the concrete matrix acts as stress transfer media in arresting the cracks that are developed due to internal stresses (Yazıcı *et al.* 2007, Bentur *et al.* 1990).

Mode-I fracture behavior of concrete was intensively studied by several researchers considering numerous mixture parameters like water content and aggregate size (Petersson 1980,

---

\*Corresponding author, Professor, E-mail: [nagasatish123@gmail.com](mailto:nagasatish123@gmail.com)

Hillerborg 1985). The properties of matrix and inclusions significantly effect on the Mode-I fracture behavior (Amparano *et al.* 2000). From an intensive beam testing of about 700 beams, Hillerborg (1985) analyzed the effect of maximum aggregate size on the Fracture energy and indicated that  $G_f$  tends to increase while MAS increases from 8 mm to 20 mm. Similar observations were reported by Mihashi *et al.* (1991), Walsh (1972), Bazant and Oh (1983) and Zhao *et al.* (2008), Zhou *et al.* (1995) conducted experiments on the effect of various MAS on the fracture properties of high strength concrete and reported that  $G_f$  increases with increase of MAS. However, some researchers have reported the opposite tendency. Bar *et al.* (1986) and wolinski *et al.* (1987) have conveyed a conflicting trend stating that there is no monotonic effect of MAS on fracture toughness values for mixes with MAS from 5 mm to 20 mm and 8 mm to 32 mm. Mihashi *et al.* (1991) exhibited that the fracture process zone (FPZ) is mostly influenced by the aggregate size. Yan *et al.* (2001) reported that the fractal dimension of Concrete greatly advances with increasing MAS. An increase in fracture properties with inclusion of Steel fibers in concrete was reported by few researchers (Antonio *et al.* 2012, Bencardino *et al.* 2010, Zhang Jun 2004) as testified from their works.

In view of the above, studies on the effect of both i.e. MAS and inclusion of fiber on fracture parameters of concrete are very limited. In this paper an attempt has been made to study the effect of volume fraction of fiber and maximum aggregate size on mode-I fracture parameters of high strength concrete.

## 2. Fracture parameters

Size effect Method (SEM) is the simplest methods to determine the fracture parameters of concrete. The Size effect method was proposed by Bazant and Pfeiffer (1987). In this method, fracture parameters are determined by three-point bending test on geometrically similar notched beams with varying sizes. Based on this method, nominal strength of geometrically similar concrete specimen can be described by size effect law as

$$\sigma_N = \frac{Bf_t}{\sqrt{1+\beta}}; \text{ Where } \beta = d/d_0 \quad (1)$$

Where,  $\sigma_N$ =Nominal stress,  $f_t$ =direct tensile strength of concrete

B and  $d_0$  are constants;  $d$  is the depth of the beam and  $\beta$  is the brittleness number.

Eq. (1) can be algebraically transformed to a linear regression equation i.e.,  $Y = AX+C$ , in which:  $X=d$ ,  $Y=(f_t/\sigma_N)^2$ ,  $B=1/\sqrt{C}$  and  $d_0=C/A$

The fracture energy ( $G_f$ ) and the effective length of Fracture Process Zone ( $C_f$ ) was obtained from the slope of the Regression line (A) and the elastic modulus (E) as given below (Bazant 1990)

$$G_f = \frac{g(\alpha)}{EA} \times f_t^2 \quad (2)$$

$$C_f = \frac{g(\alpha)}{g'(\alpha)} d_0 \quad (3)$$

$g(a)$  is the non-dimensional energy release rate and  $g'(a)$  is the derivative of  $g(a)$  with respect

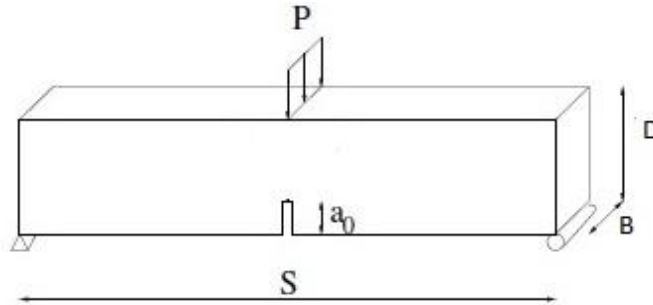


Fig. 1 Schematic view of beam setup

to the relative initial cracklength

$$\text{Where } g(\alpha) = \pi \alpha f(\alpha)^2 \tag{4}$$

In which the expression  $f(\alpha)$  was adopted from RILEM TC 89 FMT(1990)and was given by

$$f(\alpha) = \frac{1.99 - \alpha(1 - \alpha)(2.15 - 3.93\alpha + 2.7\alpha^2)}{(\sqrt{\pi})(1 + 2\alpha)(1 - \alpha)^{3/2}} \text{ for beams having geometry of } S/D = 4. \tag{5}$$

### 3. Experimental program

The Experimental program was designed to study the variation of Mode-I fracture parameters of concrete for different aggregate sizes and different volume fraction of steel fiber. This program consists of four series, namely  $D_n/d/0$ ,  $D_n/d/0.5$ ,  $D_n/d/1$  and  $D_n/d/1.5$ . In this series ‘D’ represents High strength concrete of M70 grade concrete, ‘d’ represents depth of the specimen i.e., 75 mm(Small),150 mm(Medium) and 300(Large) and ‘n’ represents the maximum aggregate size used in the mix i.e., ‘n’ equal to one that represents the maximum aggregate size is 10 mm, ‘n’ equal to two that represents the maximum aggregate size is 16 mm, ‘n’ equal to three that represents the maximum aggregate size is 20 mm. 0,0.5,1 and 1.5 represents percentage of volume fraction of steel fiber. In this investigation, for each series of beams there are three different sizes of the beams were used i.e., 350 mm×100 mm×75 mm (span is 300 mm), 650 mm×100 mm×150 mm (span is 600 mm) and 1250 mm×100 mm×300 mm (span is 1200) such that to maintain the geometrical similarity of the cross section of all the beams. The ratio of the span to the depth of the beam (S/D) was 4 for all the specimens. Fig. 1 shows the schematic representation of the beam specimen subjected to three point bending.

#### 3.1 Material details

Crimped steel fibers of 0.35 mm mean diameter and 35 mm in length (Aspect ratio is 70) were used in this investigation. Ordinary Portland cement (OPC) of 53 grade conforming to ASTM C150 Type1 with specific gravity of 3.15 was used in concrete mix; natural river sand with specific gravity 2.60 meeting the requirements of ASTM C-33 was also used as fine aggregate in the entire investigation. Crushed coarse aggregates of size 20 mm, 16 mm and 10 mm were used for the casting of specimens. To achieve the desired workability for M70 mix naphthalene

Table 1 Detail of specimens

Grade of concrete	Size of aggregate	Specimen	Length, L, (mm)	width, b, (mm)	Depth,d, (mm)	Span,S, (mm)	Notch Depth (a <sub>0</sub> )	a <sub>0</sub> /d	S/d
M70	10 mm	Small	350	100	75	300	11.25	0.15	4
		Medium	650	100	150	600	22.5	0.15	4
		Large	1250	100	300	1200	45	0.15	4
	16 mm	Small	350	100	75	300	11.25	0.15	4
		Medium	650	100	150	600	22.5	0.15	4
		Large	1250	100	300	1200	45	0.15	4
	20 mm	Small	350	100	75	300	11.25	0.15	4
		Medium	650	100	150	600	22.5	0.15	4
		Large	1250	100	300	1200	45	0.15	4

sulphonate type super plasticizer (CONPLAST SP337) was used. The dosage of super plasticizer was 8 ml/kg (by the weight of binder). In order to achieve high strength parameters additional fine materials were used such as thirteen percentage of weight of cement was replaced by silica fume and seven percentage of weight of cement was replaced by GGBS (Ground Granulated Blast Furnace Slag).

### 3.2 Casting

Cubes of 150 mm size were used to determine the compressive strength of concrete. Cylinders of 150 mm diameter and 300 mm length were used to determine the splitting tensile strength of concrete. Specially made steel moulds were used for casting beams. The moulds were tightly fitted and all the joints were sealed by Plaster of Paris in order to prevent leakage of cement slurry through the joints. Fibers were added manually to the concrete after all the other material components had been mixed together for at least 3 minutes. The compaction was done by using needle vibrator. All the specimens were water cured for 28 days. After the curing period, the test specimens were dried and provided with a notch of depth conforming to 'a<sub>0</sub>/D' ratio of 0.15 by using concrete cutter. The specimen sizes used in the present study are shown in Table 1. In this experimental investigation a total of one hundred and eight beam specimens were casted.

### 3.3 Test setup and testing procedure

All the notched concrete specimens were tested on the loading frame of capacity 100 tons under the three point bending test. The beam specimen was kept at the center of loading frame. Beam specimens were put on roller supports exactly under the center of load point in such a way that the load was applied on the axis of the specimen was carefully aligned at the center of the loading frame. The load was applied without shock and increased continuously at a constant rate until the resistance of the specimen to the increased load breaks down and no greater can be sustained. The maximum load applied on the specimen was recorded. The Crack Mouth Opening Displacement (CMOD) was measured with a dial gauge and the central deflection ( $\delta$ ) of the specimen was measured with a Linear Variable Differential Transformer (LVDT). The photograph



Fig. 2 Photograph of beam setup

Table 2 Mechanical properties of concrete

Grade of concrete	Size of aggregate	Mix Proportion	% of steel fiber	28 days compressive strength $f_{ck}$ (N/mm <sup>2</sup> )	Split tensile strength $f_t$ (N/mm <sup>2</sup> )
M70	10 MM	0.265:1:1.214:1.17	0	79.3	5.75
			0.5	83.2	6.1
			1	88.8	6.8
			1.5	92.05	7.2
	16 MM	0.25:1:1.346:1.108	0	78.4	5.8
			0.5	81	6.2
			1	86.8	7.2
	20 MM	0.24:1:1.346:1.103	1.5	95	7.1
			0	78.17	5.3
			0.5	80.4	5.8
			1	84.53	6.3
				1.5	91.9

of testing setup of beam specimen is shown in Fig. 2. To find out the mechanical properties of concrete, three cubes, three cylinders and six prisms were casted for each series of the specimens and tested. The average values of the mechanical properties of concrete and mix proportions are given in Table 2.

#### 4. Test results and discussions

For all specimens the fracture occurred by a single crack developed at the notch tip and progressed vertically towards the load point. The plain concrete specimens were certainly broken into two halves exactly over the notch (Fig. 8). The fractured specimens reinforced with steel

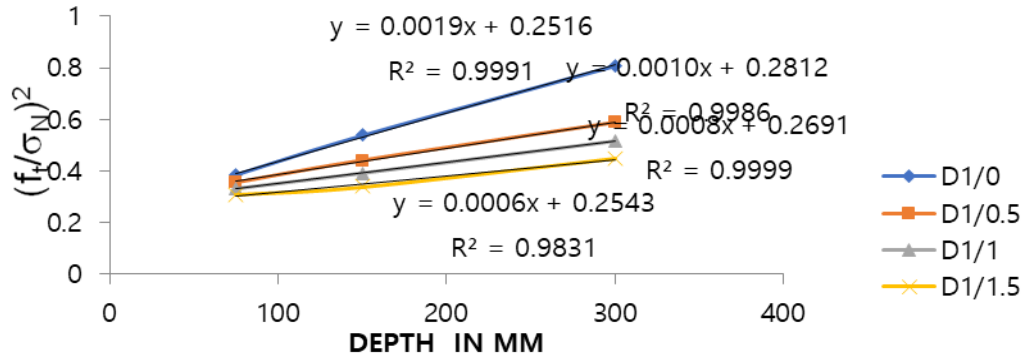


Fig. 3 Regression graph for D1 series specimens

fibers were not separated due to the fact a bridging up action by steel fibers at the cracks. This concludes, with the inclusion of steel fibers in concrete, a better mechanical integrity is accomplished during failure thereby enhancing the overall performance of concrete. For defining the mode-I fracture parameters with the help of equation (1), linear regression plots were prepared and presented the regression plot for the D<sub>1</sub>-series specimen in Fig. 3. The linear regression is

plotted for size (d) on X-axis against  $\left(\frac{f_t}{\sigma_N}\right)^2$ . The regression equation is in the form of  $Y=C+AX$ .

The characteristic size of the tested specimens is reported as  $d_0=C/A$  and the numerator in size effect law  $B=C^{-1/2}$ .  $f_t$  is the direct tensile strength of concrete, generally is assumed as 0.665 times the split tensile strength of concrete in the absence of test data (Neville 1995).  $\beta = \frac{d}{d_0}$ , indicates

the brittleness factor which characterizes the brittleness of the member. The characteristic dimension of the concrete member ( $d_0$ ) is defined as the size of the member, beyond that size LEMF principles can be applied i.e., the failure takes place like a pure brittle fracture. The nonlinear fracture mechanics is valid and should be applied for  $0.1 < \beta < 10$  (Ricardo *et al.* 2006). Quasi-brittle structures (RILEM TC QFS 2004) are those at which  $0.1 \leq \beta \leq 10$ . If  $\beta < 0.1$  then the failure may be analyzed on the basis of the strength criterion and if  $\beta > 10$  then the failure may be analyzed according to LEMF (Bazant 1986). The fracture energy, brittleness number, failure stress and fracture process zone were determined and reported in Table 3.

The utmost progressive consequence of fiber inclusion has been witnessed in energy absorption. The increase in fracture energy with increasing fiber volume fraction curtails from a great number of fibers forming a bridge in the crack and more tortuous crack propagation path. The fracture energy of 1.5% fiber reinforced concrete is about five times higher than the plain concrete for 20 mm MSA. This significant increase in fracture energy can be attributed to the ability of the steel fibers to arrest cracks at both micro- and macro-levels. At micro-level fibers inhibit the initiation of cracks, while at macro-level fibers provide effective bridging. The variation of fracture energy with maximum size of aggregate and volume fraction of fiber is presented in Fig. 4. It is concluded from this graph that the increase in maximum size of aggregate upturns the fracture energy demonstrating the behavior of the concrete member with higher MSA possessing more fracture energy than a concrete member with less MSA. This is due to the fact that presence

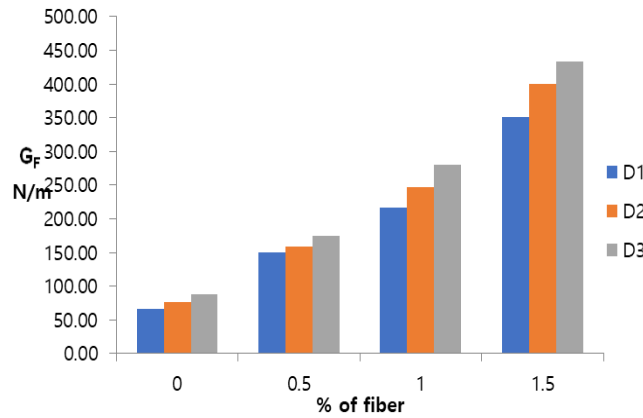


Fig. 4 Fracture Energy Vs% of Steel Fibers

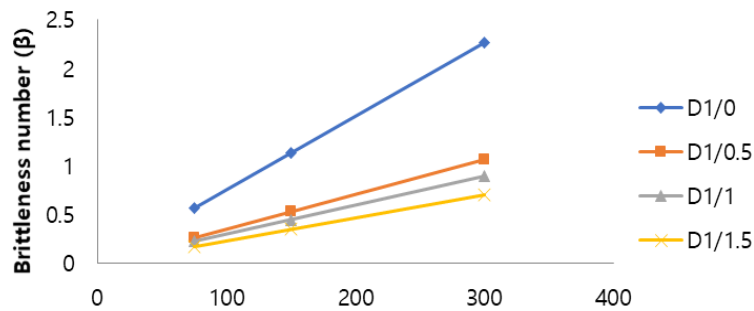


Fig. 5 Brittleness Number Vs Depth for D1 series specimens

of aggregate in cement paste matrix increases tortuosity of the fracture path. In the other words, when the concrete is under load, cracks prefer to pass weak zones such as interface transition zone (ITZ) and huge paste pores. As the aggregate size increases, the fracture path becomes more tortuous and a higher energy is required to overcome the strength of ITZ and thus fracture energy is increased. But there is no notable change in the ratio of the fracture energy of 1.5% to the plain concrete when maximum aggregate size increases from 10 mm to 20 mm. This is may be due to higher fracture energy is essential to overcome the bridging effect of fibers rather than the strength of ITZ.

Load is plotted as a function of mid-span deflection curves and crack mouth opening displacement (CMOD) curves of notched prismatic beams, and presented in Figs. 6 and 7 respectively. In the present study, we found that with an increase in MSA, A significant drop in the characteristic dimension  $d_0$  is perceived resulting in increased brittleness of the member. In other words, it can be stated that members of higher size of MSA will fail in a brittle fracture mode, even though the actual dimensions of the member being small. Fig. 5 depicts the variation of brittleness number with MSA and volume fraction of fiber. As expected, the inclusion of fibers resulted in decreasing brittleness number, representing that concrete turn out to be more ductile. Load carrying capacity, deflection correspond to ultimate load and CMOD of plain concretes increased expressively with the increase of fiber volume fraction. However, at constant fiber dosage, load carrying capacity and CMOD of composites increases with increase the size of aggregate.

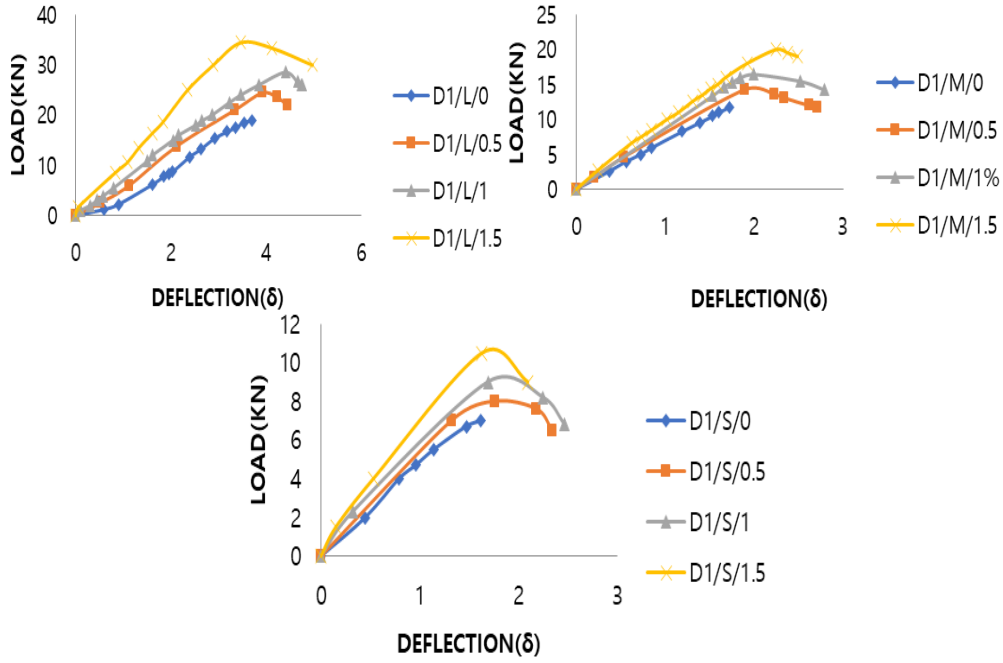


Fig. 6 Load Vs Midspan Deflection of D1 series specimens

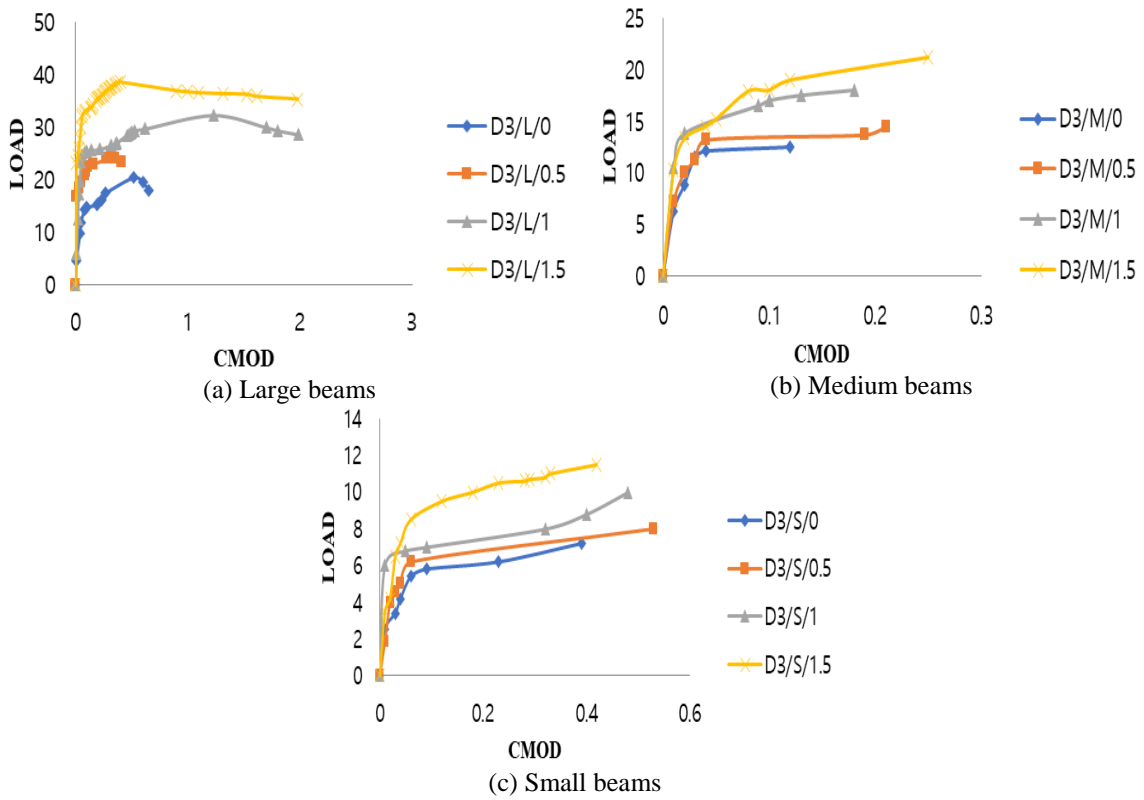


Fig. 7 Load Vs Midspan Deflection of D3 series specimens



Table 3 Fracture parameters

Beam	Failure Load (P)kN	Failure Stress N/mm <sup>2</sup>	Brittleness Number ( $\beta$ )	Fracture Energy (N/m)	Cohesive Fracture Zone(C <sub>F</sub> ) (mm)
D <sub>1</sub> /S/0	7	5.625	0.566		
D <sub>1</sub> /M/0	11.8	4.766	1.133	67.01	15.23
D <sub>1</sub> /L/0	19	3.890	2.266		
D <sub>1</sub> /S/0.5	8	6.426	0.267		
D <sub>1</sub> /M/0.5	14.3	5.768	0.533	150.35	32.35
D <sub>1</sub> /L/0.5	24.5	4.993	1.067		
D <sub>1</sub> /S/1	9	7.226	0.223		
D <sub>1</sub> /M/1	16.5	6.648	0.446	216.25	38.70
D <sub>1</sub> /L/1	28.5	5.793	0.892		
D <sub>1</sub> /S/1.5	10.5	8.426	0.177		
D <sub>1</sub> /M/1.5	20	8.048	0.354	351.22	48.76
D <sub>1</sub> /L/1.5	34.5	6.993	0.708		
D <sub>2</sub> /S/0	7.2	5.785	0.495		
D <sub>2</sub> /M/0	12	4.846	0.990	76.13	17.43
D <sub>2</sub> /L/0	19.8	4.050	1.980		
D <sub>2</sub> /S/0.5	7.7	6.186	0.340		
D <sub>2</sub> /M/0.5	14.2	5.728	0.680	155.6	36.47
D <sub>2</sub> /L/0.5	24.2	4.933	1.359		
D <sub>2</sub> /S/1	9.5	7.626	0.208		
D <sub>2</sub> /M/1	17.2	6.928	0.415	247.76	41.58
D <sub>2</sub> /L/1	30.3	6.153	0.830		
D <sub>2</sub> /S/1.5	10.3	8.266	0.162		
D <sub>2</sub> /M/1.5	18.8	7.568	0.324	385.46	62.51
D <sub>2</sub> /L/1.5	34.8	7.053	0.648		
D <sub>3</sub> /S/0	7.2	5.785	0.421		
D <sub>3</sub> /M/0	12.5	5.046	0.842	87.52	20.50
D <sub>3</sub> /L/0	20.5	4.190	1.684		
D <sub>3</sub> /S/0.5	8	6.426	0.233		
D <sub>3</sub> /M/0.5	14.5	5.848	0.466	163.48	37.03
D <sub>3</sub> /L/0.5	25.2	5.133	0.932		
D <sub>3</sub> /S/1	10	8.026	0.195		
D <sub>3</sub> /M/1	18	7.248	0.389	280.92	44.36
D <sub>3</sub> /L/1	32.3	6.553	0.778		
D <sub>3</sub> /S/1.5	11.5	9.226	0.160		
D <sub>3</sub> /M/1.5	21.2	8.528	0.320	433.07	53.98
D <sub>3</sub> /L/1.5	38.5	7.793	0.639		



Fig. 8 Specimens after testing

## 5. Conclusions

Based on the experimental results of this investigation, the following conclusions have been drawn:

- The maximum aggregate size and volume fraction of steel fibers have a significant role in fracture behavior of steel fiber reinforced concrete.
- The increase in the maximum size of aggregate increases the fracture energy i.e., the concrete with higher MSA has larger fracture energy than concrete with less MSA. The fracture energy strongly affected by both maximum aggregate size and volume fraction of fiber.
- Brittleness member increases with increase the maximum aggregate size and decrease the volume fraction of fiber i.e., decrease the MSA and inclusion of fiber in matrix makes the structure to behave in a ductile manner.
- Considering the range of brittleness number obtained in this study, it can be concluded that steel fiber reinforced concrete members with different maximum aggregate sizes must be designed using the nonlinear fracture mechanics.
- Post-cracking behaviour was mainly influenced by the amount of fibres. Post cracking response was observed for all specimens and it was increased with increasing volume of fibre.
- Effective length of cohesive fracture process zone (cf) increases with increase the maximum

aggregate size and increases with the volume fraction of fiber.

## Acknowledgments

This research work is carried out under the financial assistance from AICTE, New Delhi under RPS scheme. The authors are very thankful to the AICTE, New Delhi and also authorities of Bapatla Engineering College, Bapatla, for providing facilities for carrying out this work.

## References

- Amparano, F.E., Xi, Y. and Roh, Y.S. (2000), "Experimental study on the effect of aggregate content on fracture behavior of concrete", *Eng. Fract. Mech.*, **67**(1), 65-84.
- Caggiano, A., Cremona, M., Faella, C., Lima, C. and Martinelli, E. (2012), "Fracture behavior of concrete beams reinforced with mixed long/short steel fibers", *J. Conbuildmat.*, **37**, 832-840.
- Caggiano, A., Cremona, M., Faella, C., Lima, C. and Martinelli, E. (2012), "Fracture behavior of concrete beams reinforced with mixed long/short steel fibers", *Constr. Build. Mater.*, **37**, 832-840.
- Barr, B.I.G., Hasso, E.B.D. and Weiss, V.J. (1986), "Effect of specimen and aggregate sizes up on the fracture characteristics of concrete", *J. Cement Compos. Lightw. Concrete*, **8**, 109-119.
- Bazant, Z.P. and Pfeiffer, P.A. (1987), "Determination of fracture energy from size effect and brittleness number", *ACI Mater. J.*, **84**(6), 463-480.
- Bazant, Z.P. and Kazemi, M.T. (1990), "Determination of fracture energy, process zone length and brittleness number from size effect, with application to rock and concrete", *J. Fract.*, **44**, 111-131.
- Bazant, Z.P. and Oh, B.H. (1983), "Crack band theory for fracture of concrete", *Mater. Struct.*, **16**, 155-177.
- Bazant, Z.P., Kim, J.K. and Pfeiffer, P.A. (1986), "Nonlinear Fracture properties from size effect tests", *J. Struct. Eng.*, **112**(2), 289-306.
- Bencardino, F., Rizzuti, L., Spadea, G. and Swamy, R. (2010), "Experimental evaluation of fiber reinforced concrete fracture properties", *J. Compos.*, **41**(1), 17-24.
- Bentur, A. and Mindess, S. (1990), *Fiber Reinforced Cementitious Composites*, Elsevier Applied Science, London, New York, U.S.A.
- Hillerborg, A. (1985), "Results of three comparative test series for determining the fracture energy GF of concrete", *Mater. Struct.*, **18**, 407-413.
- Holschemacher, K., Mueller, T. and Ribakov, Y. (2010), "Effect of steel fibers on mechanical properties of high strength concrete", *J. Matdes*, **31**(5), 2604-2615.
- Mihashi, H., Nomura, N. and Niiseki, S. (1991), "Influence of aggregate size on fracture process zone of concrete detected with 3D acoustic emission technique", *Cement Concrete Res.*, **21**, 737-744.
- Neville, A.M. (2012), *Properties of Concrete*, 5th Edition, Pearson Education, Delhi, India.
- Okan, K., Erdogan, O., Cengiz, D.A., Mohamed, L. and Khandaker, M.A.H. (2016), "Effects of milled cut steel fibers on the properties of concrete", *KSCE J. Civil Eng. J.*, **20**(7), 2783-2789.
- Petersson, P.E. (1980), "Fracture energy of concrete: Practical performance and experimental results", *Cement Concrete Res.*, **10**(1), 91-101.
- Ricardo, A. and Einsfeld, M.S.L.V. (2006), "Fracture parameters of high performance concrete", *Cement Concrete Res.*, **36**, 576-583.
- RILEM FMT-89 (1990), "Size-effect method for determining fracture energy and process zone size of concrete", *Mater. Struct.*, **23**(6), 461-465.
- RILEM TC QFS (2004), "Quasi-brittle fracture scaling and size effect-final report", *Mater Struct.*, **37**, 547-568.
- Walsh, P.F. (1972), "Fracture of plain concrete", *Ind. Concrete J.*, **46**, 469-476.

- Wolinski, S., Hordijk, D.A., Reinhardt, H.W. and Cornelissen, H.A.W. (1987), "Influence of aggregate size on fracture mechanics parameters of concrete", *J. Cement Compos. Lightw. Concrete*, **9**, 95-103.
- Yan, A., Wu, K.R., Zhang, D. and Yao, W. (2001), "Effect of fracture path on the fracture energy of high-strength concrete", *Cement Concrete Res.*, **31**, 1601-1606.
- Yazıcı, S., Inan, G. and Tabak, V. (2007), "Effect of aspect ratio and volume fraction of steel fiber on mechanical properties of SFRC", *J. Conbuildmat.*, **21**(6), 1250-1253.
- Zhang, J. and Victor, C.L. (2004), "Simulation of crack propagation in fiber reinforced concrete by fracture mechanics", *J. Cemconres*, **34**, 333-339.
- Zhao, Z., Kwon, S.H. and Shah, S.P. (2008), "Effect of specimen size on fracture energy and softening curve of concrete: Part I. Experiments and fracture energy", *Cement Concrete Res.*, **38**, 1049-1060.
- Zhou, F.P., Barr, B.I.G. and Lydon, F.D. (1995), "Fracture properties of high strength concrete with varying silica fume content and aggregates", *Cement Concrete Res.*, **25**, 543-552.

JK